Paper- IM-15-10099R

Title: Quantitative assessment of flame stability through image processing and spectral analysis

Authors: Duo Sun[1]
Gang Lu[1, *]
Hao Zhou[2]
Yong Yan[1]
Shi Liu[3]

Address: [1.] Instrumentation, Control and Embedded Systems Research Group
School of Engineering and Digital Arts
University of Kent
Canterbury
Kent CT2 7NT
UK

Tel: +441227823706 (Dr Gang Lu)
Email: sunduo_0606@hotmail.com, g.lu@kent.ac.uk, and y.yan@kent.ac.uk

[2.] State Key Laboratory of Clean Energy Utilization
Institute for Thermal Power Engineering
Zhejiang University
Hangzhou, 310027,
P. R. China

Tel: +86-571-87952598
E-mail: zhouhao@cmee.zju.edu.cn

[3.] State Key Laboratory of Alternate Electrical Power System with Renewable Energy Sources
North China Electric Power University
Changping District
Beijing 102206
P. R. China

Tel: +86-10-61778520
E-mail: liushidr@yahoo.com

* Corresponding author

Abstract

This paper investigates experimentally two generalized methods, i.e., a simple universal index and oscillation frequency, for the quantitative assessment of flame stability at fossil-fuel-fired furnaces. The index is proposed to assess the stability of flame in terms of its color, geometry, and luminance. It is designed by combining up to seven characteristic parameters extracted from flame images. The oscillation frequency is derived from the spectral analysis of flame radiation signals. The measurements involved in these two methods do not require prior-knowledge about fuel property, burner type and other operation conditions. They can therefore be easily applied for flame stability assessment without costly and complex adaption. Experiments were carried out on a 9MWth heavy-oil-fired combustion test rig over a wide range of combustion conditions including variations in swirl vane position of tertiary air, swirl vane position of secondary air, and ratio of primary air to total air. The impact of these burner parameters on the stability of heavy oil flames is investigated by using the index and oscillation frequency proposed. The experimental results obtained demonstrate the effectiveness of the methods and the importance of maintaining a stable flame for reduced NO_x emissions. It is envisaged that such methods can be easily transferred to existing flame CCTV (Closed-Circuit Television) systems and flame failure detectors in power stations for flame stability monitoring.

Keywords: flame stability, flame monitoring, digital imaging, image processing, spectral analysis, oscillation frequency, NO_x emission

Highlights

- A simple universal index is proposed for the quantitative assessment of flame stability in industrial boiler. The index assesses the stability of flame in terms of its color, geometry, and luminance.
- Experiments were carried out on a $9MW_{th}$ industrial scale heavy-oil-fired combustion test rig over a wide range of combustion conditions to demonstrate the effectiveness of the proposed index and oscillation frequency for flame stability monitoring.
- Experimental results show that the lowest NO_x emission is generally observed under the most stable flame condition, which indicates the importance of maintaining a stable flame for reduced NO_x emissions and the necessity of the flame stability assessment.
- The presented methods can be transferred easily to existing flame CCTV systems and flame failure detectors in power stations.

1. Introduction

Fossil-fuel-fired furnaces are widely used in power generation industry for electricity generation. A common problem that occurs in the furnace is the instability of the flame. The problem has become severe due to the recent trend of using low quality fuel, fuel blends and co-firing of biomass with fossil fuels. A unstable flame causes many combustion problems such as, low combustion efficiency, high NO_x emissions and furnace safety (e.g., increased wall thermal stress, and vibration of the furnace) [1]. Therefore, a reliable and effective means for the on-line continuous monitoring and quantification of flame stability is becoming increasingly crucial for maintaining the optimized performance of the furnace.

The stability of flame is a broad concept largely relating to the ignition stability of fuel, air-to-fuel ratio, the balance between the velocities of the flame and air-fuel mixture, and the thermal-acoustic stability between the heat release and acoustic oscillations [2, 3]. The ultimate aim of retaining the flame stability in a combustion system is to achieve optimized combustion process, i.e., high combustion efficiency, low pollutant emissions (e.g., NOx) and safe plant operation. Significant research has been conducted to investigate the mechanism and characteristics of flame instability [4-6] theoretically and experimentally by using various monitoring diagnostic methods such as Laser Induced Fluorescence [7], infrared absorption [8] and CCD (Charge-Coupled Device) cameras [9, 10]. A great deal of efforts have also been devoted to the study of flame stability limit [11] and diagram [12-14], which generally correspond to a specific fuel and burner, and gives the range of controllable parameters (e.g., equivalence ratio, fuel stream velocity and heat input rate) within which blow-off and flashback can be avoided for a safety purpose. However, very limited work focused on the quantitative assessment of the flame stability for industrial combustion applications, which is an essential step to advanced flame monitoring and diagnostics, and thus combustion optimization. The technical challenges are thought to lie in two aspects. Firstly, there is currently no well-defined criterion about the flame stability as well as on-line assessment method in the combustion domain, even though an unstable flame has been identified as one of main causes of many combustion problems for decades. This is mainly ascribed to the fact that a flame is a three-dimensional thermo-fluid-dynamic field associated with many combustion phenomena including heat, light, sound, pressure, and so on. This nature of flame has led to the investigation of the flame stability through different perspectives. It also gives rise to the difficulty, if not impossibility, in comprehensively defining flame stability by a single or a few parameters. Regardless of the nature of the flame sensorial data that are available to a flame monitoring system (e.g., planar laser induced fluorescence images, chemiluminescence images, pyrometry-derived temperature maps, or non-filtered images), it is very challenging to establish a methodology to process those data to quantify the stability of the flame. Secondly, difficulties are associated with practical issues including the accessibility of the furnace for a flame monitoring system and the protection of such a system from the high temperature and fouling in the furnace [15]. These practical issues give rise to considerable constrains in applying some of flame diagnostic techniques, such as laser-based systems, to long-term routine operation in a power station environment [16].

The techniques that are currently available for flame monitoring at power stations are limited, mainly flame failure detectors and CCTV systems, due to a number of factors such as restricted access, harsh environment, high cost, and safety reasons. Flame failure detectors are based on ultraviolet, visible or infrared sensing, and capture flame radiation signals. However, these detectors can indicate only flame presence or absence for safety purposes, though they are equipped in most of furnaces as a compulsory device. Flame visualization techniques have increasingly been used as a diagnostic tool in the understanding and optimization of combustion processes, as they provide spatial and temporal information about the thermal and chemical characteristics of flames [15, 17]. Passive imaging techniques, unlike laser-based active imaging techniques, avoid the need for external illumination or seeding. They record directly the radiation emitted by the flame and have been identified as the one of the most effective flame visualization methods for industrial applications. The CCTVs, as the simplest passive imaging system, have already been installed in boilers at many power stations as an auxiliary flame monitoring technique of flame failure detection. However, CCTVs are only for general surveillance purposes and the interpretation of flame images is based on operator's experience.

A multi-functional instrumentation system for flame monitoring in industrial furnaces was developed [18, 19]. The system incorporates digital imaging and photo-detector techniques and is capable of capturing flame images and radiation signals simultaneously and producing a range of characteristic parameters of the flame on an on-line basis. Efforts have also been made to assess the flame stability through the statistical analysis of physically meaningful parameters extracted from flame images (e.g., ignition point, luminous region, brightness, non-uniformity and temperature) and through spectral analysis of flame radiation signals [19]. Although many features (parameters) can be extracted from flame images and spectral signals, however, they vary significantly from case to case and some features may be significant only under specific cases. For instance, flame ignition points can be observed only if the flame is detached from the nozzle of the burner. For an un-detached flame, the flame ignition points are not applicable. Therefore, it is critical, from a practical operation point of view, to devise more generalized criterion that can be used for assessing for the flame stability, particularly where combustion systems use different types of fuels (e.g., gas, oil, coal, and biomass), and operate under different conditions (e.g., over-fire air, flue gas recirculation and etc.).

The work presented in this paper focuses on establishing a generalized method for the quantitative assessment of the flame stability. A universal flame stability index is defined and used to assess the stability of flame in terms of its color, geometry, and luminance. The index is derived from the statistical analysis of up to seven individual characteristic parameters extracted from flame images. In [20], the concept of the flame stability index and the preliminary results of using such as concept for the flame stability assessment were firstly reported. In the paper, the thorough theory of the flame stability index and the detailed procedure of using the stability index for the flame assessment are introduced. Experiments are conducted on a $9MW_{th}$ industrial-scale heavy-oil-fired combustion test facility over a wide range of combustion conditions. The impacts of various burner parameters on flame stability are studied by the proposed index. The correlation between the flame stability and NO_x emissions is also investigated. In addition, the oscillation frequency, which was defined as a characteristic frequency of flame radiation signal [21], was suggested to be relevant with flame stability to a degree, but very limited experimental studies have been reported. In this study the oscillation frequency incooperates with the proposed stability index, forming the generalization of these two measurement approaches for the flame stability assessment.

The main contributions of this study lie in the proposed definition of the universal flame stability index, and the demonstration of this index together with the flame oscillation frequency for assessing quantitatively the flame stability under a wide range of heavy-oil-fired combustion conditions. The proposed method does not require prior-knowledge about fuel property, burner type and other operation conditions, and therefore can be easily applied for flame stability assessment without ad hoc and costly adaption for new applications. It should be stressed that the validation of the proposed approach for the quantitative assessment of the flame stability is conducted experimentally, and the mathematical modelling of flame stability is beyond the scope of this paper. It is realized that the mathematical modelling techniques such as CFD (Computational Fluid Dynamics) modelling provide very powerful tools in designing and analyzing combustion systems. However, due to a number of factors, it is still very difficult to use these modelling techniques to provide with the quantitative and reliable predication of combustion parameters, and subsequently flame stability, especially for large industrial boilers. These factors include the lack of reliable flame models, the need for high performance computational systems, the intrinsic uncertainty and variations in combustion systems and fuels burnt, the absence of a well-defined criterion about flame stability, and so on. These factors are also the main reason that the permanent supervision of flame is needed in industrial boilers.

The paper is organized as follows: Section 2 presents the detailed description of the proposed methodology for the quantitative flame stability assessment is given in. Section 3 gives the experimental results and discussion of applying the proposed technical approach for assessing the flame stability on a 9MWth heavy-oil-fired combustion test rig. Section 4 remarks the findings derived from this study and future research directions.

2. Methodology

The present work assesses the stability of a flame through the analysis of flame images and radiation signals, as flame instability generally occurs with large fluctuations in flame geometry, radiation intensity, or temperature (contained in color information). The proposed index and oscillation frequency quantify these fluctuations hence the flame stability to some degree in a relative way.

2.1 System set-up

Figure1 shows the block diagram of the flame stability assessment system. The system mainly consists of a 90° viewing-angle optical probe protected by a water-cooling jacket, a beam splitter, a 1/3 inch CMOS RGB digital camera (UI-1640SE) with 1.3-million pixels (1280H×1024V), an embedded photo-detector and signal-processing board, and a high-performance embedded-motherboard with dedicated application software. All these optical and electronic components are integrated into a single compact unit offering the system high portability and robustness. The optical probe is used to transmit the light of the flame inside the combustion chamber to the camera and photo-detector (CENTRONIC, OSD1-5T) simultaneously with the aid of the beam splitter. The flame images and radiation signals are processed to derive the proposed stability index and oscillation frequency on an online basis, by the embedded-motherboard and the signal-processing board, respectively. The results are transmitted to remote control room via Ethernet. The detailed description about the design, implementation and evaluation of the system can be found in [19].

2.2 Measurement principles

2.2.1 Definition of the flame stability index

As flame images provide valuable information on the spatial and temporal dynamics of the flame, it is naturally considered to assess the stability of flame through its images. However, apart from the characteristics of imaging system used to capture flame images, the quality and content of the obtained images are closely relevant with many application-related factors such as fuel properties, burner type, combustion condition, and system installation. These factors may vary dramatically in different cases. Therefore, it is desirable to have a generalized criterion that can be used for assessing for the flame stability under different combustion conditions. The concept of flame stability index is then proposed for this purpose. In this study, the flame stability index combines the dynamic characteristics of seven parameters derived from flame images. The seven parameters are concerned with color, geometry, and luminance. Figure 2 shows the measurement procedure of the index, which can be divided into three steps, i.e., transformation of color space, extraction of parameters, and data fusion.

2.2.1.1 Color space transformation from RGB to HSI

The first step is to transform the format of a color image from original RGB (Red, Green and Blue) to HSI (Hue, Saturation and Intensity). The color characteristic of a flame is closely linked with the flame emission spectra and largely dependent on the fuel properties, air supply, and temperature. The flame color characteristic should therefore be taken into a consideration when evaluating the flame stability. The RGB color space is useful for color display, where the color and intensity are inseparably stored in the three primary color components. However, the R, G, and B components in the RGB space are highly correlated [22]. When the intensity changes, all the three components will change accordingly. It is therefore not good for color analysis. The HSI model is another commonly used color space in image processing, in which the color information of an image is separated from its intensity information. The Hue (H) component represents the dominant wavelength in the spectral distribution of light wavelengths, indicating basic colors. The Saturation (S) component is a measure of the purity of the color, denoting the amount of white light mixed with the hue. The Intensity (I) component is determined by the amount of light, describing the brightness of the image [22].

The HSI color model can be described geometrically as in Figure 3. The H component describes the color in the form of an angle between a reference line and the color point. The range of the H value is generally from 0° to 360°; for example, red is 0°, yellow is 60°, green is 120°, and magenta is 300°. For the convenience of analysis, the H value is normalized by 360° in the present study. The S component represents the perpendicular distance from the color point to the axis. The range of S component is [0, 1]. The nearer the point is to the center axis, the lighter is the color. The I component is the height of the color point in the axis direction, ranging from 0 to 1 where 0 represents black and 1 means white. Each slice perpendicular to the axis is a plane with the same intensity.

The HSI coordinates can be transformed from the RGB space as follows:

$$H = \begin{cases} \cos^{-1}\left\{\frac{\frac{1}{2}[(R-G)+(R-B)]}{[(R-G)^2+(R-B)(G-B)]^{1/2}}\right\}/360^o, & \text{if } B \le G \\ 1-\cos^{-1}\left\{\frac{\frac{1}{2}[(R-G)+(R-B)]}{[(R-G)^2+(R-B)(G-B)]^{1/2}}\right\}/360^o, & \text{if } B > G \end{cases} \tag{1}$$

$$S = 1 - \frac{3}{R+G+B} \cdot \left[\min\left(R, G, B\right)\right], \tag{2}$$

$$I = \frac{R+G+B}{3}. \tag{3}$$

2.2.1.2 Extraction of parameters

The second step is to derive flame parameters from HSI images. Seven parameters, assigned as M_H, M_S, M_I, C_H, C_S, C_I, and A_I, are extracted. M_H, M_S, and M_I denote the mean values of

H, S and I components, respectively, whilst C_H, C_S, and C_I are the contrast values of the three components. A_I represents the flame area, which is derived from I image.

The mean M_k and contrast C_k (pixel) of an image are defined as (4) and (5), respectively,

$$M_k = \frac{1}{P\times Q}\sum_{i=0}^{P-1}\sum_{j=0}^{Q-1} V_k(i, j), \tag{4}$$

$$C_k = \left(\frac{1}{P\times Q}\sum_{i=0}^{P-1}\sum_{j=0}^{Q-1}\left(V_k(i, j) - M_k\right)^2\right)^{1/2}, \tag{5}$$

where k=H, S, I, and $V_k(i, j)$ is the i-th j-th element of the two dimensional image with a size P×Q pixels.

The flame area, A_I (pixel^2), is determined by applying an appropriate threshold (estimated from the maximum background noise) to the I image, i.e.,

$$A_I = \frac{1}{P\times Q}\sum_{i=0}^{P-1}\sum_{j=0}^{Q-1}\begin{cases}1, \text{if } V_I(i, j) > \text{threshold} \\ 0, \text{other}\end{cases}. \tag{6}$$

2.2.1.3 Data fusion

The last step is to fuse the standard deviations of the extracted parameters to derive the universal stability index (δ) in the form as,

$$\delta = \prod_{i=1}^{7}\left(\frac{\phi(P_i) - \sigma_{P_i}}{\phi(P_i)}\right)^{w_i} \in [0, 1], \tag{7}$$

where $P_i \in \{M_H, M_S, M_I, C_H, C_S, C_I, A_I\}$, and σ_{Pi} is the standard deviation of P_i. $\phi(P_i)$ is the theoretical maximum standard deviation of P_i and is used to limit the index boundary to [0, 1]. w_i is the weight for P_i. In the present work, the same weight w_i=2 was assigned for all the parameters, which means that all flame parameters are taken as equally important. In a specific case, a larger weight can be given to the parameter that is more important than others.

It should be note that although quantities P_i possess different physical meanings, they are normalized by their theoretical maximums, and so the normalized quantities are dimensionless and have the same range [0, 1]. After normalization, these quantities are combined in such a form of (7) that, if there is any large variation in any of these quantities, which indicates the unstable flame, it will be indicated by this combined index.

The theoretical maximum standard deviation of a variable *x*, $\phi(x)$, depends on the dynamic range and probability distribution of *x*. Suppose $x = \{x_i | i = 1,2,...N, x_i \in [L_1, L_2]\}$ with a unknown probability distribution, the mean and standard deviations of x are denoted as μ_x and σ_x, respectively,

$$\mu_x = \tfrac{1}{N}\sum_{i=1}^{N} x_i \ , \tag{8}$$

$$\sigma_x = \left(\tfrac{1}{N}\sum_{i=1}^{N} \left(x_i - \mu_x\right)^2 \right)^{1/2} . \tag{9}$$

Rearranging (9) yields

$$\sigma_x = \left(\tfrac{1}{N}\sum_{i=1}^{N} \left(x_i - \tfrac{L_2 - L_1}{2}\right)^2 - \left(\mu_x - \tfrac{L_2 - L_1}{2}\right)^2 \right)^{1/2} . \tag{10}$$

Considering $\frac{1}{N}\sum_{i=1}^{N} \left(x_i - \frac{L_2 - L_1}{2}\right)^2 \geq \left(\mu_x - \frac{L_2 - L_1}{2}\right)^2 \geq 0$ yields

$$\sigma_x \leq \left(\tfrac{1}{N}\sum_{i=1}^{N} \left| x_i - \tfrac{L_2 - L_1}{2} \right|_{\max}^2 \right)^{1/2} \leq \tfrac{L_2 - L_1}{2} . \tag{11}$$

The maximum value of $\frac{L_2-L_1}{2}$ is achieved if and only if $\mu_x = \frac{L_2-L_1}{2}$ and $x_i = 0$ or $\frac{L_2-L_1}{2}$ for *i=1, 2,…, N*. In other words, the theoretical maximum standard deviation of *x*, $\phi(x)$, equals to a half of the dynamic range, i.e.,

$$\phi(x) = \frac{L_2 - L_1}{2}. \tag{12}$$

The dynamic ranges of H, S, and I are [0, 1], determining that $\phi(M_H)$, $\phi(M_S)$, $\phi(M_I)$ and $\phi(A_I)$ are 0.5, while $\phi(C_H)$, $\phi(C_S)$ and $\phi(C_I)$ are 0.25.

The features of the proposed index are summarized as follows. Firstly, the index evaluates the stability of a flame through analyzing dynamics of its color, luminance and geometry. Secondly, the index has a fixed boundary, ranging from 0 to 1, which is desirable in metrology. The highest value ‘1’ is achieved if and only if all parameters are constant with time, indicating a perfectly stable state. The lowest value ‘0’ occurs when the standard deviation of any parameter reaches its theoretical maximum value, indicating an extremely unstable state. Last but not least, the index is computationally simple, suitable for on-line measurement. The measurement procedure does not depend on fuel properties, furnace types, or combustion conditions, and thus can be applied to new applications without any ad-hoc and costly adaption.

2.2.2 Spectral analysis and oscillation frequency

As can be observed by human eye, most flames exhibit certain spatial and temporal dynamic patterns. The dynamic patterns can be revealed to a degree in the power spectrum of flame radiation signals to give an indication about the stability of a flame. Previous studies have suggested that the low frequency components of flame signals could be ascribed to flame geometrical fluctuations due to aerodynamic or convective effect, whilst high frequency components could be due to the energy transitions among intermediate radicals or variations in the energy emission rate of reacting species [23]. In the present work, it was hoped that the spectral analysis of flame signals can be used to provide an insight into the validity of the proposed stability index.

The power spectral density (PSD) of a flame radiation signal can be derived from

$$P(f) = \tfrac{1}{N_1}\left(X_{N_1}(f)\right)^2, \qquad (13)$$

where $P(f)$ is the PSD estimate, and $X_{N_1}(f)$ is the Fourier Transform of N_1-point sampling data sequence $X_{N_1}(f)$ of the signal. The data length N_1, for Fast Fourier Transform, is 1024 in this study.

The oscillation frequency of flame was proposed previously [21] as a characteristic frequency of the PSD and suggested to be relevant with flame stability. It is defined as the power-density weighted average frequency over the entire frequency range, i.e.,

$$F = \frac{\sum_{i=1}^{N_2} p_i \cdot f_i}{\sum_{i=1}^{N_2} p_i}, \qquad (14)$$

where F is the oscillation frequency, f_i is the i_{th} frequency, p_i is the power density of the i_{th} frequency component, and N_2 is the number of frequency components. The effectiveness of using the oscillation frequency as a quantitative flame stability indicator is investigated experimentally in the following section.

3. Experimental Results and Discussions

Experimental work was undertaken on a $9MW_{th}$ industrial-scale heavy-oil-fired combustion test facility, as illustrated in Figure 4. The furnace is equipped a single low NO_x burner in a horizontal cylindrical combustion chamber with 11 meters in length and 1.3 meters in diameter [19]. Heavy oil was atomized by steam and injected into the combustion chamber through an oil gun, and then mixed with surrounding primary air (PA), secondary air (SA), and tertiary air (TA) successively. The flame imaging system penetrated the furnace through a side port close to the front wall (Figure 4) to visualize the root part of the flame as the central reaction zone. A wide range of combustion conditions were created, including variations in the swirl vane position of the tertiary air, the swirl vane position of the secondary air, and the ratio of the primary air to total air. The impacts of these burner parameters on the stability of heavy oil flames are investigated. During all these tests, the total air flow rate (9100Nm^3/h) and the oil flow rate (800kg/h) were kept constant. The NO_x emissions of flue gas were measured concurrently by a gas analyzer during the tests.

3.1 Effects of the swirl vanes on flame stability

The swirling of air flow affects considerably the intermixing of the atomized oil fuel and air flow hence the flame stability and combustion performance. The adjustable settings of the combustion test facility that are capable of controlling the swirling of air flow include the swirl vane angle of the TA and the swirl vane position of the SA.

The TA swirl vane angle determines the direction of the tertiary air flow. It is defined as the angle between the swirl vane and the plane perpendicular to the burner axis, varying from 0°

(air inlet fully closed) to 90° (air inlet fully open but without any swirl). Under the same air flow rate, a smaller swirl angles gives a stronger swirling intensity. Three different angles, 25°, 35°, and 45°, were created during the test. Figure 5 shows the typical example of instantaneous flame images for different TA swirl vane angles.

The effects of the TA swirl vane angle on the flame stability were previously investigated in [19] in terms of geometrical, luminous and fluid-dynamic characteristics. Some of the results are briefly re-presented here for comparison with the results from the proposed index and for completeness of the study. It was previously found that a TA swirl vane angle 25° resulted in significantly increased amplitude of low frequency components (Figure 6b) and decreased oscillation frequency (Figure 6c) [19], indicating great geometrical fluctuation and decreased flame stability. The result from measured flame stability index is consistent with this finding, as shown in Figure 6a. The stability index increased gradually with the vane angle, which confirms that an increased TA swirl vane angle would result in improved flame stability. The lowest stability index is observed at 25°, indicating the flame is relatively unstable under such a swirl vane angle setting.

The SA swirl vane position controls the amount of air going through the SA swirl vane. For the SA, part of the air flow goes through the swirl vane, and the rest bypasses the swirl vane and goes straightforward into the combustion chamber. The lower the swirl vane position, the more air goes through the swirl vane, and the stronger the swirling intensity. During the test, three different SA swirl vane positions, i.e., -17mm, 30mm and 65mm, were created. Figure 7 shows the typical example of instantaneous flame images for the different SA swirl vane positions. A direct comparison among the images has suggested that a greater SA swirl vane position resulted in a slightly stretched flame, similar to the effect of a greater TA swirl vane angle. This can be understood by the fact that the stronger the swirling intensity of the secondary air, the more air goes swirly towards away from the burner axis due to the effect of centrifugal force, resulting in a wide spread angle of the flame.

Figure 8a shows the stability indices at SA swirl vane positions -17mm and 30mm are relatively low, indicating an unstable flame under these two conditions. The highest stability index is observed at 65mm, indicating an improved flame stability. This result is supported by the power spectral analysis and NO_x emissions. The increase of the SA swirl vane position gave rise to increased amplitudes in both the low- and high-frequency components (Figure 8b), suggesting that the SA swirl vane position has a significant impact on both the geometrical and kinetic characteristics of the flame. Figure 8d shows that the lowest NO_x emission was observed at the stability-improved condition, which is consistent with the result obtained from the TA swirl vane angle test (Figure 6d). It should also be noted that under this test the flame stability index gives a better indication than the oscillation frequency. As can be seen in Figure 8c, the oscillation frequency failed to indicate the variations in the flame stability caused by a change in the SA swirl vane position. This is due to the intrinsic limitation imposed by the definition of the oscillation frequency as the weighted average frequency over the whole spectrum.

3.2 Effects of the ratio of primary air to total air on flame stability

The purpose of this test was to investigate the impacts of the spatial distribution of air flow on the flame stability. During the test, the ratio of the SA to total air (SA ratio) (43%) provided for the burner was kept constant. When the PA ratio increased, the TA ratio decreased by the same degree correspondingly. Five different PA ratios, i.e., 11%, 14%, 17%, 20% and 23%

were tested. Figure 9 shows the typical instantaneous images of the flame under different PA ratios.

Figure 10a shows the variations of the measured stability index with the PA ratio. With the increase of the PA ratio, the index increased gradually, indicating an improved stability. The lowest value is obtained at PA 11%, indicating the flame is comparatively less stable under such a PA ratio. This result is in line with the spectral analysis, as illustrated in Figure 10b. The much higher amplitude of the low-frequency components, which results in the lowest oscillation frequency among the five tested conditions (Figure 10c), is observed at PA 11%, indicating an increased geometrical fluctuation and decreased instability at such a condition. The highest NO_x emission also emerged at PA 11% (Figure 10d) and decreased gradually with the PA ratio, implying that the improved flame stability gave rise to lower NO_x emissions.

3.3 Correlations between flame stability and NO_x

In the above experiments, for a specific test, the lowest NO_x emission is generally observed under the most stable flame condition. To investigate further this phenomenon, data were collected from a wider range of combustion conditions including variations in overfire air to total air ratio and injection position [24]. Under all the conditions, the oil flow rate and the total air flow rate were kept constant for a fair comparison. Figure 11a gives the comparison between the measured flame stability index and corresponding NO_x emissions during all the tests. It is evident that the volume of NO_x emissions in the flue gas decreases gradually with an improved flame stability. This finding is also supported by the results of the oscillation frequency (as show in Figure 11b), which shows low NO_x emissions were achieved generally with a high oscillation frequency, indicating a better flame stability. The results presented show the importance of maintaining a stable flame and the necessity of the flame stability assessment. It should be mentioned that the results do not imply that flame stability can be used directly as a predictor of NO_x emissions, as the NO_x formation process is also dependent upon many other factors. However, they exemplify the potentials of using the proposed technique for assessing the performance of combustion system.

The above experiments (Section 3.1-3.3) demonstrated the effectiveness of the two methods in flame stability assessment. Although the results obtained are preliminary, they are very promising. It can be seen that the two methods can give an indication about the variation of flame stability with different conditions. More importantly, the results from these two different methods are well matched and they gave similar conclusions regarding the trend of NO_x emission with flame stability, which are consistent with past experience. The advantage of these two methods together with the imaging system also lies in its practicality and feasibility for use in large scale industrial boilers, which is difficult to achieve when using some other flame diagnostic techniques.

4. Conclusions

This paper attempts to devise generalized methods for the quantitative assessment of flame stability in industrial furnaces. A simple universal index, which is derived from the statistical analysis of flame images and assesses the stability of flame in terms of its color, geometry and luminance, has been proposed. The advantages of this index include a fixed range [0, 1] desirable in metrology, and simple computation complexity suitable for on-line processing. The experimental results, obtained under a wide range of combustion conditions on a $9MW_{th}$

heavy-oil-fired combustion test facility, have demonstrated the effectiveness of the index for the quantitative assessment of flame stability. In addition, the feasibility of the oscillation frequency derived from the flame radiation signal as a simple quantitative indicator of flame stability has also been demonstrated. One important advantage of the index proposed and the oscillation frequency is the generalization of their measurement approaches. This is particularly useful because the concept can potentially be transferred to existing flame CCTV systems and flame detectors in power stations without a costly and complex adaption, This is due to the fact that the flame images captured by the CCTV systems and the flame radiation signals captured by the flame detectors should carry most information which the flame imaging system provide and thus can be used to compute the stability index and oscillation frequency for the quantitative assessment of flame stability. Last but not least, for all different sets of tests, the lowest NO_x emission has generally been observed when the flame is most stable, which indicates the importance of maintaining a stable flame for reduced NO_x emissions. Future research will be directed towards the usage of the technique as an indication or prediction for flame stability problems such as increased wall thermal stress, vibration of the furnace, low combustion efficiency, and high NO_x emissions, and the integration of the technique into industrial boiler control system.

Acknowledgment

Acknowledgements are made to the Research Councils UK (RCUK) for providing a grant (EPSRC, EP/F061307/1) in aid of this research. This work is also supported by the Biomass Fossil Fuel Research Alliance (Project #2), The Royal Academic Engineering (Ref12/13RECI046) and 111 Talent Introduction Projects (B12034 and B13009) at North China Electric Power University.

References

[1] A. Fichera, C. Losenno, and A. Pagano, "Experimental analysis of thermo-acoustic combustion instability," *Applied Energy*, vol. 70, pp. 179-191, 2001.

[2] S. Su, J. H. Pohl, D. Holcombe, and J. A. Hart, "Techniques to determine ignition, flame stability and burnout of blended coals in p.f. power station boilers," *Progress in Energy and Combustion Science*, vol. 27, pp. 75-98, 2001.

[3] S. Candel, "Combustion dynamics and control: Progress and challenges," *Proceedings of the Combustion Institute*, vol. 29, pp. 1-28, 2002.

[4] T. Lieuwen, H. Torres, C. Johnson, and B. T. Zinn, "A mechanism of combustion instability in lean premixed gas turbine combustors," *Journal of Engineering for Gas Turbines and Power*, vol. 123, pp. 182-189, 2001.

[5] S. Seo, "Combustion instability mechanism of a lean premixed gas turbine combustor," *Journal of Mechanical Science and Technology*, vol. 17, pp. 906-913, 2003.

[6] K. K. Venkataraman, L. H. Preston, D. W. Simons, B. J. Lee, J. G. Lee, and D. A. Santavicca, "Mechanism of combustion instability in a lean premixed dump combustor " *Journal of Propulsion and Power*, vol. 15, pp. 909-918, 1999.

[7] Y. Wu, Y. Lu, I. S. Al-Rahbi, and G. T. Kalghatgi, "Prediction of the liftoff, blowout and blowoff stability limits of pure hydrogen and hydrogen/hydrocarbon mixture jet flames," *International Journal of Hydrogen Energy*, vol. 34, pp. 5940-5945, 2009.

[8] J. G. Lee and D. A. Santavicca, "Experimental diagnostics for the study of combustion instabilities in lean premixed combustors," *Journal of Propulsion and Power*, vol. 19, pp. 735-750, 2003.

[9] X. Paubel, A. Cessou, D. Honore, L. Vervisch, and R. Tsiava, "A flame stability diagram for piloted non-premixed oxycombustion of low calorific residual gases," *Proceedings of the Combustion Institute,* vol. 31, pp. 3385-3392, 2007.

[10] D. Y. Kiran and D. P. Mishra, "Experimental studies of flame stability and emission characteristics of simple LPG jet diffusion flame," *Fuel,* vol. 86, pp. 1545-1551, 2007.

[11] M. S. Mansour, "Stability characteristics of lifted turbulent partially premixed jet flames," *Combustion and Flame,* vol. 133, pp. 263-274, 2003.

[12] C. Lee, C. Hwang, and S. Hong, "Proposal and validation of a new type of flame stability diagram for partially premixed flames," *Fuel,* vol. 87, pp. 3687-3693, 2008.

[13] C. Lee and C. Hwang, "An experimental study on the flame stability of LFG and LFG-mixed fuels," *Fuel,* vol. 86, pp. 649-655, 2007.

[14] C. Hwang, S. Lee, J. Kim, and C. Lee, "An experimental study on flame stability and pollutant emission in a cyclone jet hybrid combustor," *Applied Energy,* vol. 86, pp. 1154-1161, 2009.

[15] J. Ballester and T. Garcı´a-Armingol, "Diagnostic techniques for the monitoring and control of practical flames," *Progress in Energy and Combustion Science,* vol. 36, pp. 375-411, 2010.

[16] G. Lu, Y. Yan, and M. Colechin, "A digital imaging based multifunctional flame monitoring system," *IEEE Transactions on Instrumentation and Measurement,* vol. 53, pp. 1152-1158, 2004.

[17] K. Kohse-Höinghaus, R. S. Barlow, M. Aldén, and J. Wolfrum, "Combustion at the focus: laser diagnostics and control," *Proceedings of the Combustion Institute,* vol. 30, pp. 89-123, 2005.

[18] D. Sun, G. Lu, and Y. Yan, "An embedded imaging and signal processing system for flame stability monitoring and characterisation," in *IEEE International Conference on Imaging Systems and Techniques*, 2010, pp. 210-213.

[19] D. Sun, G. Lu, H. Zhou, and Y. Yan, "Flame stability monitoring and characterization through digital imaging and spectral analysis," *Measurement Science and Technology*, vol. 22, p. 114007, 2011.

[20] D. Sun, G. Lu, H. Zhou, X. Li, and Y. Yan, "A simple index based quantitative assessment of flame stability," in *IEEE International Conference on Imaging Systems and Techniques*, Beijing, China, 2013, pp. 190 - 193.

[21] Y. Huang, Y. Yan, G. Lu, and A. Reed, "On-line flicker measurement of gaseous flames by images processing and spectral analysis," *Measurement Science and Technology*, vol. 10, pp. 726-733, 1999.

[22] H. Cheng, X. Jiang, Y. Sun, and J. Wang, "Color image segmentation: advances and prospects," *Pattern Recognition*, vol. 34, pp. 2259-2281, 2001.

[23] A. R. Jones, "Flame failure detection and modern boilers," *Journal of Physics E: Scientific Instruments*, vol. 21, pp. 921-928, 1988.

[24] D. Sun, G. Lu, H. Zhou, and Y. Yan, "Measurement of soot temperature, emissivity and concentration of a heavy-oil flame through pyrometric imaging," in *IEEE International Conference on Instrumentation and Measurement Technology*, 2012, pp. 1865-1869.

List of Figures' Captions

Figure 1. Block diagram of the flame stability assessment system.

Figure 2. Measurement procedure of the stability index.

Figure 3. HSI color space.

Figure 4. Layout of the test furnace and the system installation.

(a) Layout of the test furnace.

(b) System installation.

Figure 5. Flame images taken for different swirl vane angles of tertiary air.

(a) 25° (b) 35° (c) 45°

Figure 6. Variations of flame characteristics with swirl vane angles of tertiary air.

(a) Stability index.

(b) Power spectral density estimates [19].

(c) Oscillation frequency [19].

(d) NO_x emissions [19].

Figure 7. Flame images taken for different swirl vane positions of secondary air.

(a) -17mm (b) 30mm (c) 65mm

Figure 8. Variations of flame characteristics with swirl vane position of secondary air.

(a) Stability index

(b) Power spectral density estimates.

(c) Oscillation frequency.

(d) NO_x emissions.

Figure 9. Flame images taken for different ratios of primary air to total air.

(a) 11% (b) 14% (c) 17%

Figure 10. Variations of flame parameters with the ratio of primary air total air.

(a) Stability index.

(b) Power spectral density estimates.

(c) Oscillation frequency.

(d) NO_x emissions.

Figure 11. Variations of NO_x emissions with flame stability index and oscillation frequency.

(a) Flame stability index.

(b) Oscillation frequency.

List of Figures

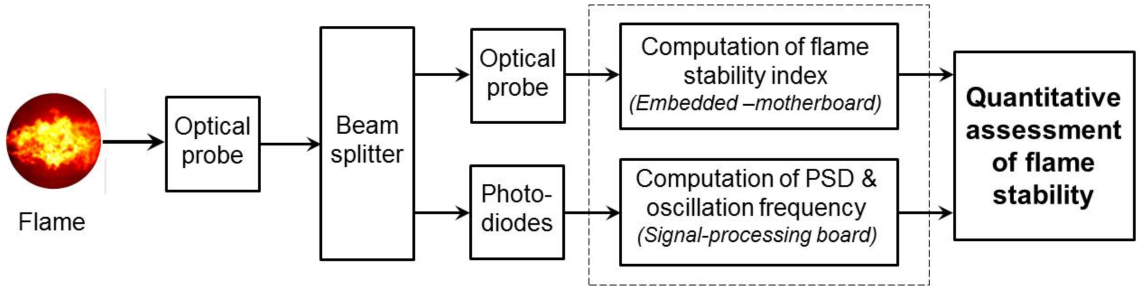

Figure 1

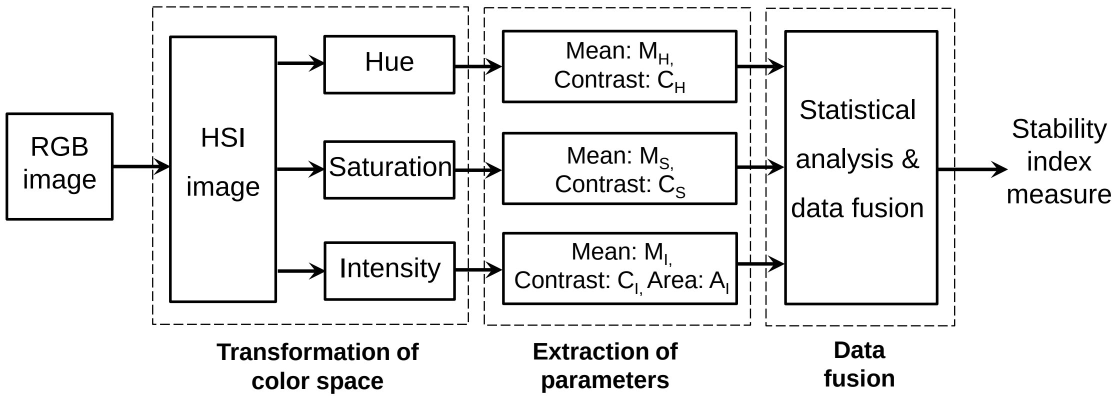
RGB image
HSI image
Hue
Saturation
Intensity
Mean: $M_{H,}$ Contrast: C_H
Mean: $M_{S,}$ Contrast: C_S
Mean: $M_{I,}$ Contrast: $C_{I,}$ Area: A_I
Statistical analysis & data fusion
Stability index measure
Transformation of color space
Extraction of parameters
Data fusion

Figure 2

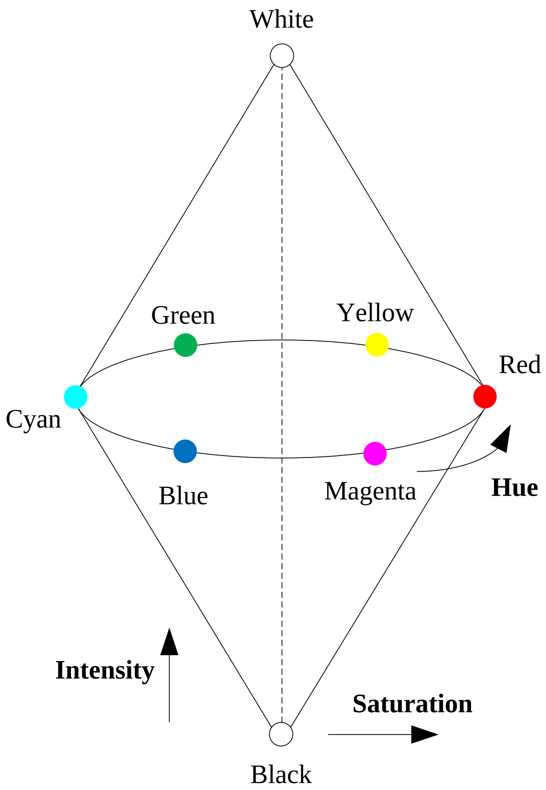
White
Green
Yellow
Red
Cyan
Blue
Magenta
Hue
Intensity
Saturation
Black

Figure 3

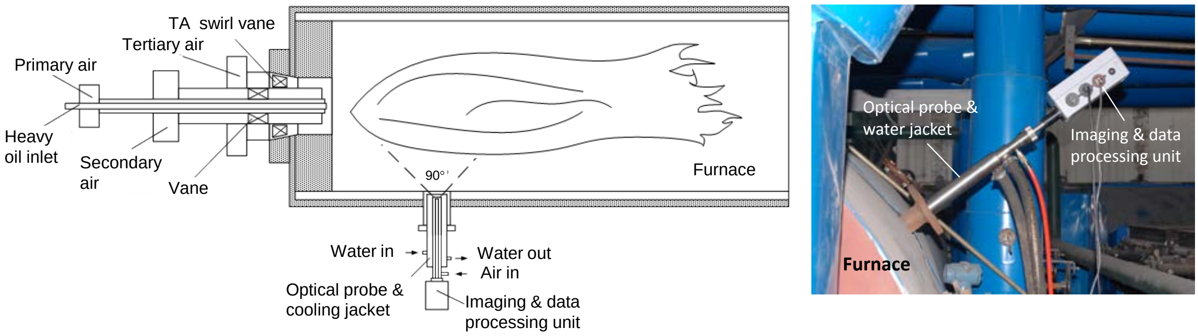
TA swirl vane
Tertiary air
Primary air
Heavy oil inlet
Secondary air
Vane
Furnace
90°
Water in
Water out
Air in
Optical probe & cooling jacket
Imaging & data processing unit
Optical probe & water jacket
Imaging & data processing unit
Furnace

(a) (b)

Figure 4

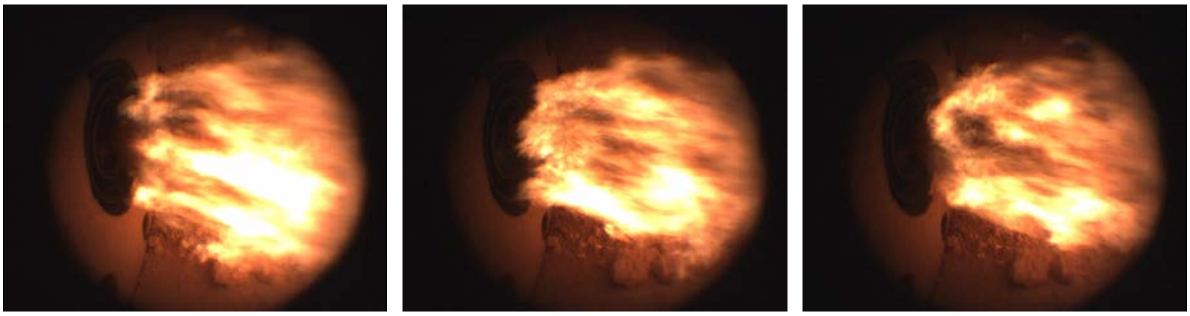

(a) (b) (c)

Figure 5

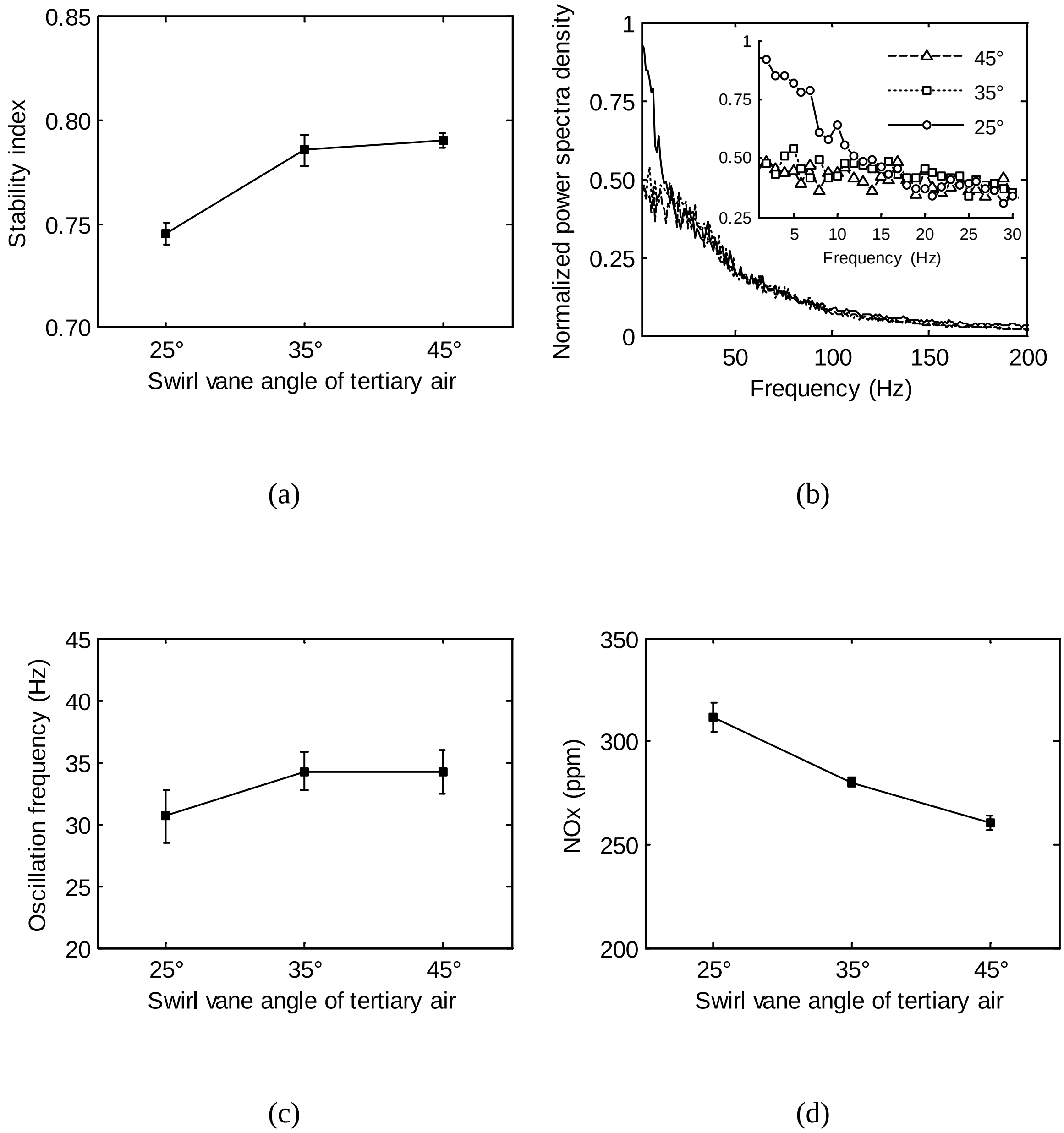
Stability index
Swirl vane angle of tertiary air
(a)
Normalized power spectra density
Frequency (Hz)
45°
35°
25°
(b)
Oscillation frequency (Hz)
Swirl vane angle of tertiary air
(c)
NOx (ppm)
Swirl vane angle of tertiary air
(d)

Figure 6

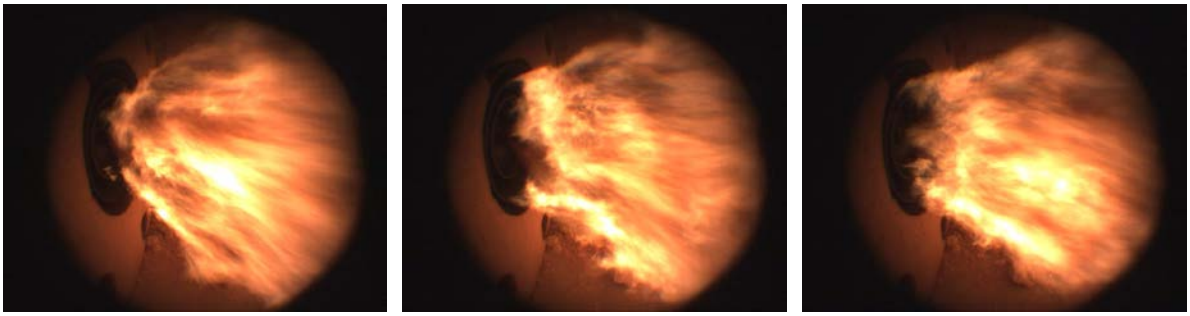

(a) (b) (c)

Figure 7

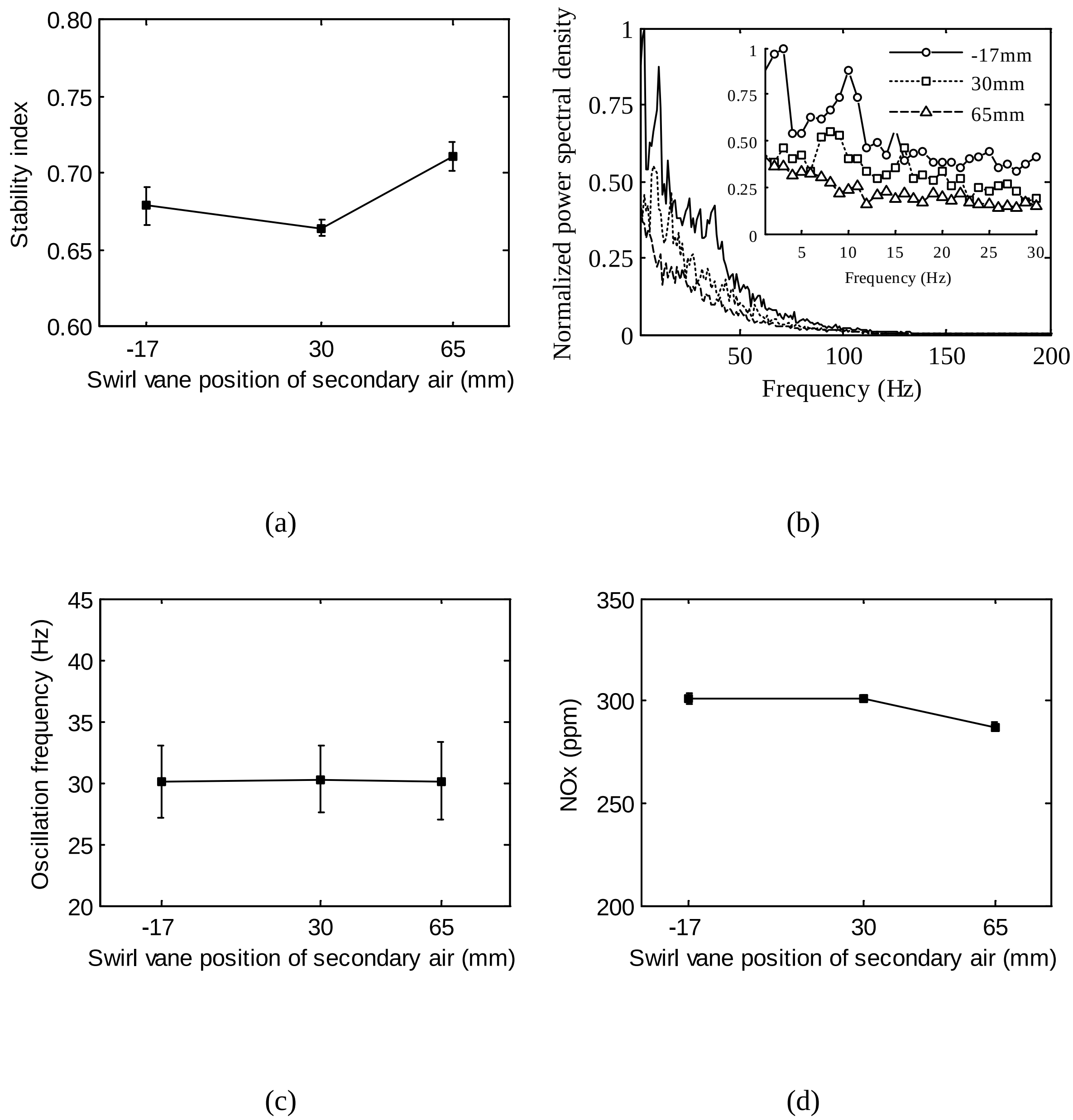
Stability index
0.80
0.75
0.70
0.65
0.60
-17
30
65
Swirl vane position of secondary air (mm)
(a)
Normalized power spectral density
1
0.75
0.50
0.25
0
50
100
150
200
Frequency (Hz)
-17mm
30mm
65mm
5
10
15
20
25
30
(b)
Oscillation frequency (Hz)
45
40
35
30
25
20
-17
30
65
Swirl vane position of secondary air (mm)
(c)
NOx (ppm)
350
300
250
200
-17
30
65
Swirl vane position of secondary air (mm)
(d)

Figure 8

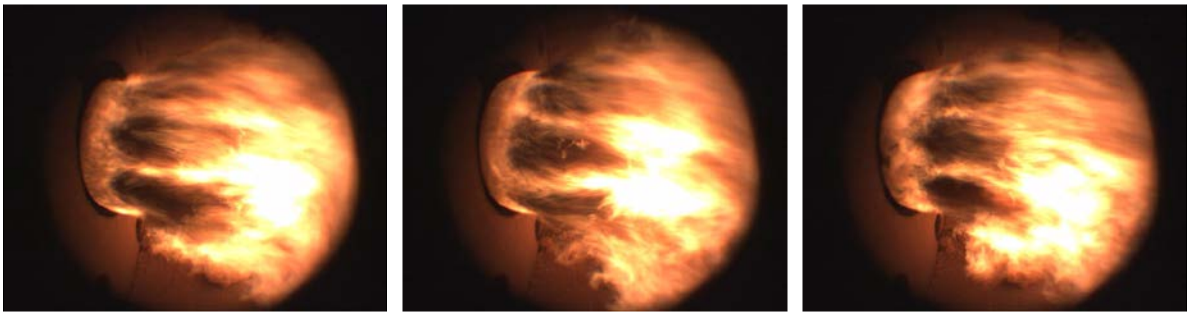

(a) (b) (c)

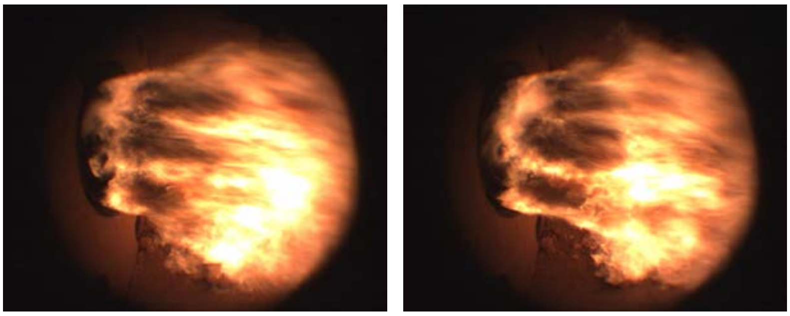

(d) (e)

Figure 9

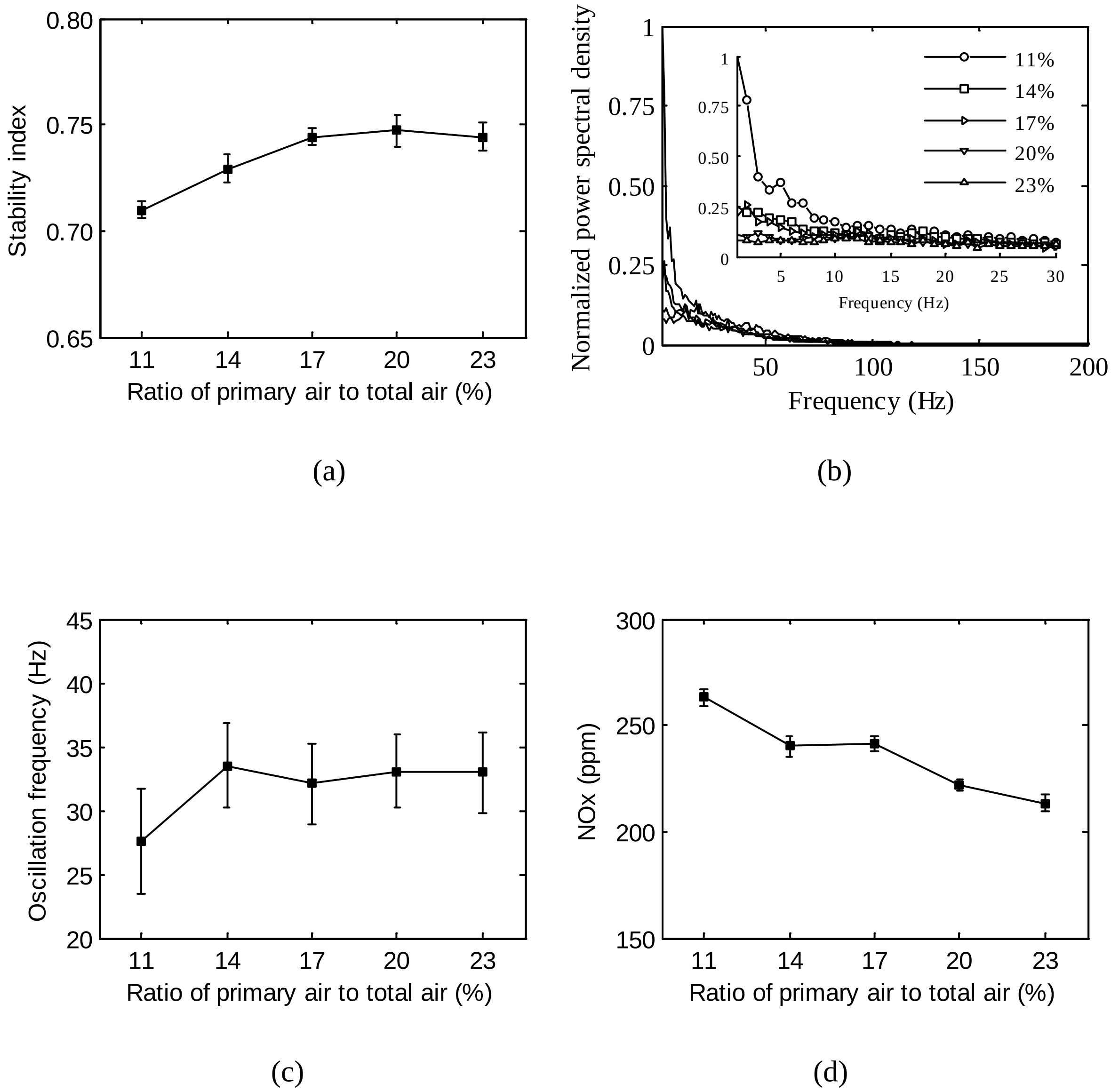

Stability index
0.80
0.75
0.70
0.65
11
14
17
20
23
Ratio of primary air to total air (%)
(a)
Normalized power spectral density
1
0.75
0.50
0.25
0
50
100
150
200
Frequency (Hz)
11%
14%
17%
20%
23%
5
10
15
20
25
30
(b)
Oscillation frequency (Hz)
45
40
35
30
25
20
Ratio of primary air to total air (%)
(c)
NOx (ppm)
300
250
200
150
Ratio of primary air to total air (%)
(d)

Figure 10

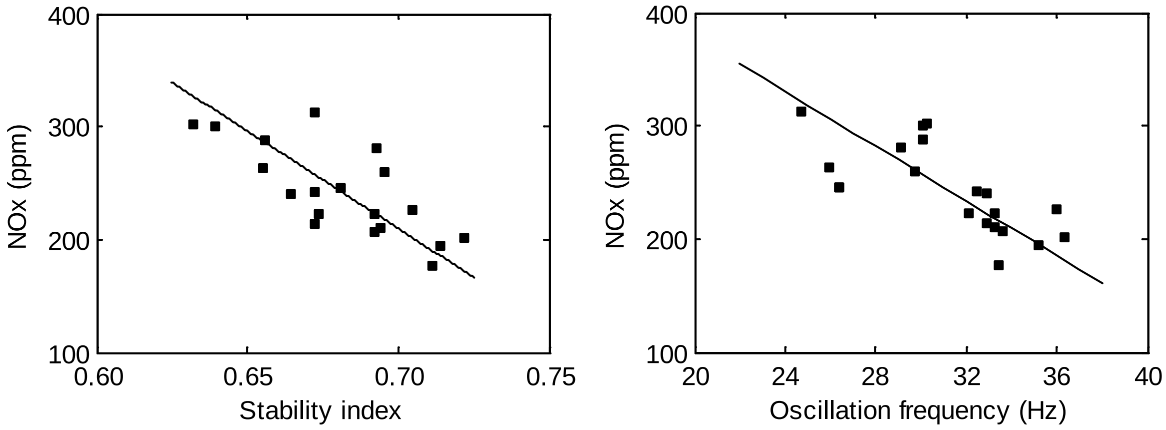
400
300
200
100
NOx (ppm)
0.60
0.65
0.70
0.75
Stability index
400
300
200
100
NOx (ppm)
20
24
28
32
36
40
Oscillation frequency (Hz)

(a) (b)

Figure 11